Comprehensive steady state analysis of bidirectional dual active bridge DC/DC converter using triple phase shift control

Harrye, Yasen A.; Ahmed, K.H.; Adam, G.P.; Aboushady, A.A.

Published in:
2014 IEEE 23rd International Symposium on Industrial Electronics (ISIE)

DOI:
10.1109/ISIE.2014.6864653

Publication date:
2014

Document Version
Peer reviewed version

Comprehensive Steady State Analysis of Bidirectional Dual Active Bridge DC/DC Converter Using Triple Phase Shift Control

Yasen A. Harrye, K.H Ahmed & G.P Adam
School of Engineering
University of Aberdeen
Aberdeen, U.K
Email: yasen.harrye@abdn.ac.uk

A.A Aboushady
Electrical & Control Engineering Department
Arab Academy for Science & Technology
Alexandria, Egypt
Email: ahmed.aboushady@ieee.org

***Abstract*— Several papers have been published recently on TPS control of dual active bridge (DAB) converter, however, no complete study of the converter operation behaviour exists, that takes into account all switching modes in both charging and discharging (bidirectional) power transfer. In this paper, six switching modes and their complements with opposite power transfer direction are defined with their operational constraints. Exact expressions for power transferred are derived with no fundamental frequency assumptions and range of power transfer for each mode is also defined to characterize mode limitations. Detailed constraints for zero voltage switching (ZVS) are also obtained. A new definition for converter reactive power consumption is introduced. This is based on calculation of inductor apparent power which avoids fundamental frequency approximations as well as the vague negative (back flowing) power definitions in recent papers. All known DAB phase shift modulation techniques including conventional, dual and extended phase shift, represent special cases from triple phase shift, therefore the presented analysis provides a generalised theory for all phase shift based modulation techniques.**

Keywords— Dual active bridge converter (DAB), Reactive power, Triple phase shift (TPS), Zero voltage switching (ZVS)

I. INTRODUCTION

There has been considerable interest in the development and applications of bidirectional dual active bridge converter (DAB) in recent years because of its use in existing and emerging power electronics technologies. This includes renewable energy generation, energy storage, electric vehicles, power distribution in microgrids and aircraft power distribution. Renewable energy generation and its use have been on the rise and among these prime sources is the offshore wind power generation. The most formidable challenges of this technology have been the interconnection and integration of different wind farm clusters, requiring use of dc connections mechanism [1]. Also owing to the unpredictable peak power as a result of wind speed fluctuations, energy storage means are required to store energy during high generation peaks and retrieve during low peaks. Therefore in order to transmit power from offshore wind farms to onshore for regulation, interface and integrate in a future DC grid; high power dc-dc converters are required as the main interface component.

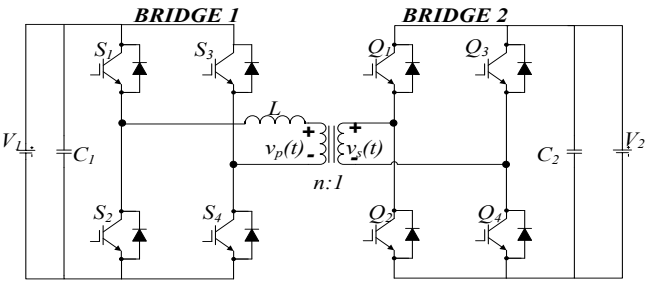

Fig. 1 DAB circuit diagram

Isolated dual active bridge (DAB) bidirectional converter which was proposed in [2], and is illustrated in Fig.1, has shown to be attractive candidate for high power dc/dc conversion due its high power density, soft switching capability, bidirectional power flow, galvanic isolation and simple control methods [2]. Use of DAB with 1MW renewable offshore wind energy has been shown [3]. Investigation of DAB converter for electric vehicles and in energy storage system has been shown to be promising [4].

Studies have been on going to analyse, design, control and improve the overall performance of DAB converter. Among these are the modulation schemes [5-7], converter losses reduction [8-10] and modelling of the converter characteristics [11- 12]. The first proposed conventional phase shift (CPS) modulation scheme [13] operates the converter bridges with full square waves while controlling the phase shift angle between them in order to determine power transferred. However, it has limitations of high inductor RMS current and hard switching at light loads under wide variations of the input and output voltages. Therefore, different modulations techniques have been published to solve aforementioned problems [5].

Dual phase shift (DPS) modulation [6] aims to reduce the converter reactive power, increase overall efficiency and during power up, suppress the transformer inrush current but has a limitation of some suboptimal modes [7]. Pulse width modulations (PWM) control of DAB converter has been

investigated in detail by [7], whereby using hybrid combinations of CPS, single PWM (SPWM) and dual PWM (DPWM), the authors have shown an improvement in low power operation of the converter in wide input output voltages, extension of ZVS range, reduction of peak and RMS currents and further reduction of the transformer size. In [8], DAB converter using PWM modulation was introduced and shown an extension of ZVS. Triple phase shift modulation was studied by [7, 14-17] to further enhance the performance of the converter in terms of improving ZVS range and reducing the overall losses by introducing an extra control variable. In [14], TPS was introduced to study the stability of DAB converter. In [15], only four TPS modes were studied to extend ZVS operating range and increase the converter efficiency. Twelve switching modes were identified by [9, 16] and analysis was performed only for some of the modes using fundamental component approximation. In [17], a multiphase shift scheme including DPS and TPS was investigated to determine optimal sub modes from the waveform features.

In this paper a comprehensive investigation of DAB converter operation is addressed. Although recently several papers have been published on TPS, complete switching modes analysis of the converter with the operational constraints has not been studied. All the operating modes are investigated with their operational constraints while deriving exact expressions for inductor currents at each switching instant. Average power transferred is calculated without using fundamental frequency approximation. Moreover, ZVS possibilities and detailed constraints for the converter bridges are determined. Reactive power, unlike recent papers defining it as back-flowing power [6, 19, 20], and papers assuming fundamental frequency analysis [21] is defined and calculated on a more accurate basis. This involves calculation of non-sinusoidal apparent power at the inductor. The analysis presented in this paper provides a generalised theory for all phase shift modulation methods since they are all a special case of TPS. This will be discussed in section four.

II. DAB TRIPLE PHASE SHIFT CONTROL

By referring the converter in Fig.1 to the transformer primary side, neglecting transformer magnetizing inductance and assuming n:1 turns ratio, DAB converter can be simplified to equivalent circuit model in Fig. 2 (a).

In TPS, three control parameters D_1, D_2 and D_3 are used. D_1 is the phase shift between switches S_1 & S_4, D_2 is the phase shift between the switches Q_1 & Q_4 while D_3 is the phase shift between S_1 & Q_1 as illustrated in Fig.2 (b).

Analysis is performed assuming lossless converter and transformer with $V_1 > nV_2$, i.e buck mode operation. Both power flow directions (charging & discharging in case DAB is connected to a battery) are studied. Analysis of boost mode operation ($V_1 < nV_2$) is identical to buck mode and will be omitted in this paper.

By referring to Fig. 2(a), the instantaneous inductor current $i_L(t)$, can be calculated using

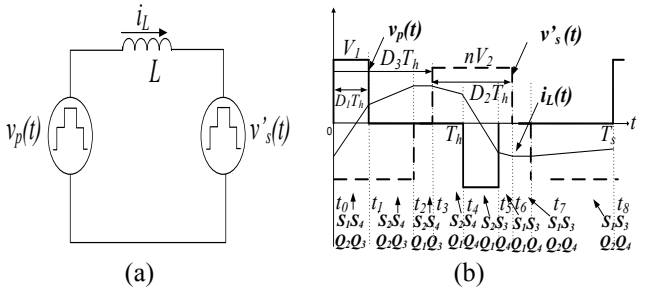

Fig.2. (a) DAB equivalent circuit referred to transformer primary side (b) voltage and currents waveforms for TPS control

$$i_L(t) = \frac{1}{L}\int_{t_n}^{t} \left(v_p(t) - v'_s(t)\right) dt + i_L(t_n) \qquad t_n \le t \le t_{n+1} \qquad (1)$$

where t_n represents n^{th} switching instant as illustrated in Fig.2(b).

Inductor currents are crucial for active and reactive power calculations, in addition to determination of ZVS constraints. This will be discussed further in section three.

III. PERFORMANCE ANALYSIS

Based on combinations of phase shifts D_1, D_2 and D_3, full, partial and no overlaps of both bridges quasi square wave voltages give rise to six switching modes and their complements, for both power flow directions using TPS. Typical operating waveforms for each of these modes are illustrated in Table I.

In order to assess the modes of operation, several performance indicators of DAB converter are investigated. Exact expressions for the inductor current are needed. Normalised inductor currents to ($1/4f_sL$), for the positive half cycle switching instants are derived and listed in Table II (where f_s is the switching frequency). Due to inductor current half-wave symmetry, negative half cycle values are omitted. These can be calculated by negating their counter positive half cycle values.

A. Power Transfer

Average power transferred by the converter can be calculated at either bridge by assuming a lossless inductor using

$$P = \frac{1}{T_h}\int_0^{T_h} v_p(t) i_L \, dt = \frac{1}{T_h}\int_0^{T_h} v'_s(t) i_L \, dt \qquad (2)$$

Per unit expression for average power normalised with respect to maximum possible transferable power by the converter is shown in Table I for each mode. Maximum power (used as the base power), is obtained with CPS at 90^0 phase shift between bridge voltages [9, 13].

$$P_{base} = \frac{nV_1V_2}{8f_sL} \qquad (3)$$

Table I: DAB modes of operation & power equations using TPS control

	Mode 1	Mode 1'	Mode 2	Mode 2'
Waveforms	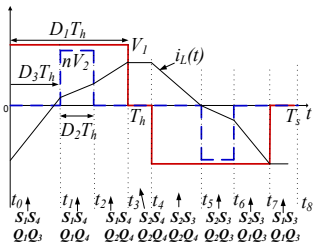	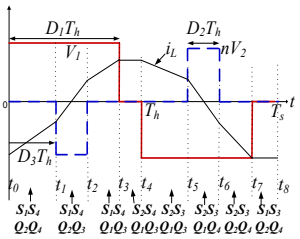	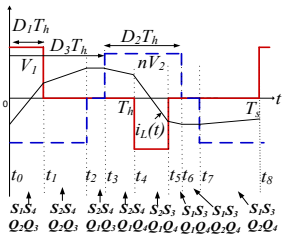	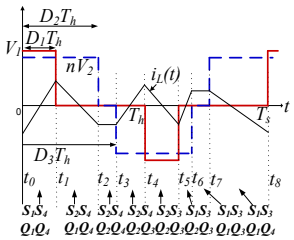
	$t_o = 0, t_1 = D_3T_h, t_2 = (D_3 + D_2)T_h, t_3 = D_1T_h, t_4 = T_h = \frac{1}{2f_s}$		$t_o = 0, t_1 = D_1T_h, t_2 = (D_2 + D_3 - 1)T_h, t_3 = D_3T_h, t_4 = T_h = \frac{1}{2f_s}$	
Mode operational constraints	$D_1 \geq D_2$ $0 \leq D_3 \leq D_1 - D_2$		$D_2 \geq D_1$ $(1 + D_1 - D_2) \leq D_3 \leq 1$	
Power & power range (pu)	$P_{pu} = 2\left[D_2^2 - D_1D_2 + 2D_2D_3\right]$ $Range: P_{\max} = 0.5pu, P_{\min} = -0.5pu$	$P_{pu} = -2\left[D_2^2 - D_1D_2 + 2D_2D_3\right]$ $Range: P_{\max} = 0.5pu, P_{\min} = -0.5pu$	$P_{pu} = 2\left[D_1^2 - D_1D_2 + 2D_1 - 2D_1D_3\right]$ $Range: P_{\max} = 0.5pu, P_{\min} = -0.5pu$	$P_{pu} = -2\left[D_1^2 - D_1D_2 + 2D_1 - 2D_1D_3\right]$ $Range: P_{\max} = 0.5pu, P_{\min} = -0.5pu$
	Mode 3	**Mode 3'**	**Mode 4**	**Mode 4'**
Waveforms	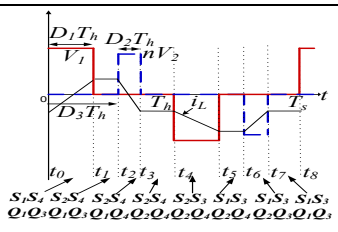	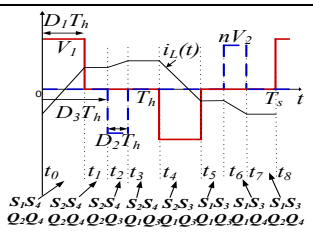	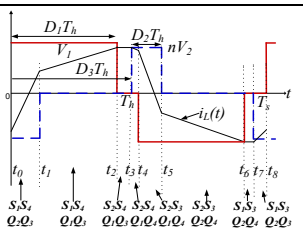	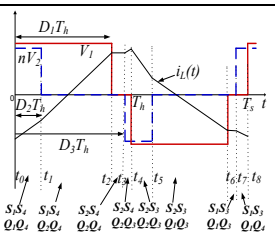
	$t_o = 0, t_1 = D_1T_h, t_2 = D_3T_h, t_3 = (D_2 + D_3)T_h, t_4 = T_h = \frac{1}{2f_s}$		$t_o = 0, t_1 = (D_2 + D_3 - 1)T_h, t_2 = D_1T_h, t_3 = D_3T_h, t_4 = T_h = \frac{1}{2f_s}$	
Mode operational constraints	$D_2 \leq 1 - D_1$ $D_1 \leq D_3 \leq 1 - D_2$		$D_1 \leq D_3 \leq 1$ $1 - D_3 \leq D_2 \leq 1 - D_3 + D_1$	
Power & power range (pu)	$P_{pu} = 2\left[D_1D_2\right]$ $Range: P_{\max} = 0.5pu, P_{\min} = 0pu$	$P_{pu} = -2\left[D_1D_2\right]$ $Range: P_{\max} = 0.0pu, P_{\min} = -0.5pu$	$P_{pu} = 2\begin{bmatrix} -D_2^2 - D_3^2 + 2D_2 + 2D_3 \\ -2D_2D_3 + D_1D_2 - 1 \end{bmatrix}$ $Range: P_{\max} = 0.67pu, P_{\min} = 0pu$	$P_{pu} = -2\begin{bmatrix} -D_2^2 - D_3^2 + 2D_2 + 2D_3 \\ -2D_2D_3 + D_1D_2 - 1 \end{bmatrix}$ $Range: P_{\max} = 0pu, P_{\min} = -0.67pu$
	Mode 5	**Mode 5'**	**Mode 6**	**Mode 6'**
Waveforms	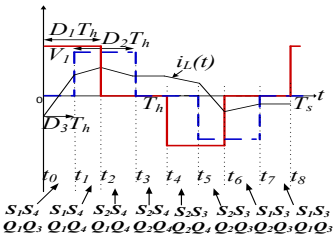	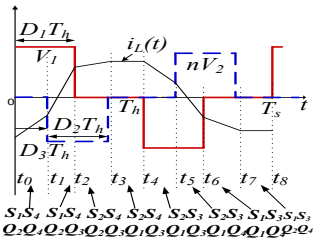	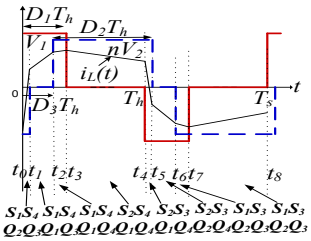	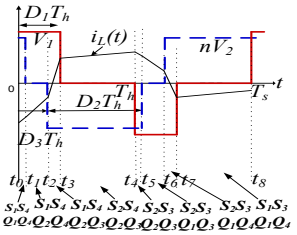
	$t_o = 0, t_1 = D_3T_h, t_2 = D_1T_h, t_3 = (D_2 + D_3)T_h, t_4 = T_h = \frac{1}{2f_s}$		$t_o = 0, t_1 = (D_2 + D_3 - 1)T_h, t_2 = D_3T_h, t_3 = D_1T_h, t_4 = T_h = \frac{1}{2f_s}$	
Mode operational constraints	$D_1 - D_3 \leq D_2 \leq 1 - D_3$ $0 \leq D_3 \leq D_1$		$1 - D_2 \leq D_1$ $1 - D_2 \leq D_3 \leq D_1$	
Power & power range (pu)	$P_{pu} = 2\left[-D_1^2 - D_3^2 + D_2D_1 + 2D_1D_3\right]$ $Range: P_{\max} = 0.667pu, P_{\min} = 0pu$	$P_{pu} = -2\left[-D_1^2 - D_3^2 + D_2D_1 + 2D_1D_3\right]$ $Range: P_{\max} = 0pu, P_{\min} = -0.667pu$	$P_{pu} = 2\begin{bmatrix} -D_1^2 - D_2^2 - 2D_3^2 + 2D_3 - 2D_2D_3 \\ +D_1D_2 + 2D_1D_3 + 2D_2 - 1 \end{bmatrix}$ $Range: P_{\max} = 1pu, P_{\min} = 0pu$	$P_{pu} = -2\begin{bmatrix} -D_1^2 - D_2^2 - 2D_3^2 + 2D_3 - 2D_2D_3 \\ +D_1D_2 + 2D_1D_3 + 2D_2 - 1 \end{bmatrix}$ $Range: P_{\max} = 0pu, P_{\min} = -1pu$

Range of power transfer for each mode is also computed to characterise mode limitations. This is done by applying the mode operational constraints to the derived power equations. The result gives the capability of converter power transfer, with respect to the full range under specific mode of operation

In complementary modes, bridge 2 waveform is shifted by 180^0 from original mode, hence resulting in the exact but negative power range. From Table I, it can be seen that modes 6 and 6' are the only modes that cover the whole converter operating power range. Modes 1, 1', 2 and 2'are capable of charging and discharging operation, but only for half the power range. Modes 3, 4, 5 and 6 with their complements only provide unidirectional power transfer capability each. Finally, it is worth noting that, in mode 3 and 3' power transfer is independent of D_3, meaning that it can be solely controlled by controlling bridge voltages.

B. ZVS Constraints

To ensure that the converter switches are operating with ZVS, anti-parallel diodes must conduct prior to switch turn on. After switch voltage drops to zero, current commutates from the anti-parallel diode to the switch enabling turn on at zero voltage, resulting in zero turn on power loss. This is a desirable converter characteristic since it enables its use in high power applications in addition to a more compact design due to use of higher switching frequency and lower electromagnetic interference.

Therefore, at the instant of switch turn on, current in the switch must be negative. This provides the condition for ZVS. With respect to the switches in Fig.1 and their respective conducting current directions, conditions for the switches ZVS can be summarised as

$$\begin{aligned} &For\ \ S_1, S_4, Q_2, Q_3 \quad i_L\big|_{t=turn\,on} < 0 \\ &For\ \ S_2, S_3, Q_1, Q_4 \quad i_L\big|_{t=turn\,on} > 0 \end{aligned} \tag{4}$$

According to (4), ZVS constraints are derived and listed in Table III. Only modes where ZVS is realisable for all switches are indicated with their constraints. Otherwise ZVS is only partially obtained for the converter, i.e. for some switches only as indicated by modes 1, 3, 3' and 5.

C. Reactive power

Reactive power is a parameter of interest to investigate in DAB converter, since by reducing reactive power consumption; RMS inductor current is minimised for a specified level of power transfer. This reduces conduction and copper losses. Reactive power loss in DAB converter has been discussed in literature [6, 18-20]. In [6, 19], authors attempt to reduce reactive power loss by introducing dual phase shift control. Unlike CPS, the transformer primary and secondary voltages are not limited to 50% duty cycles but zero states are introduced, resulting in a quasi-square waveform. In [20], reactive power is defined as back-flowing power to the converter. This is inaccurate because it means that reactive

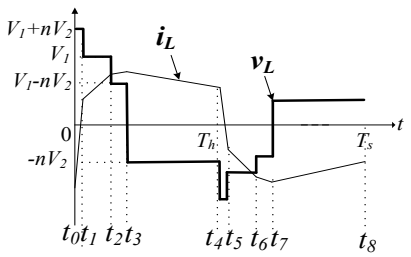

Fig.3 Inductor voltage and current waveforms for mode 6

power only occurs when voltage and current are of opposite polarity (negative power flow). So if no negative power flow exists, then converter has zero reactive power consumption. However, this is in accurate since DAB always absorbs reactive power from the converters due to coupling inductance no matter the level of power transfer. In [18], authors propose a method to minimise reactive power through design of optimal transformer turns ratio.

In this paper, a new definition of reactive power is introduced based on calculating apparent power S_L at the inductor. Since inductors do not absorb active power, the apparent power is therefore equivalent to the reactive power consumption by the inductor. This is, by definition, equivalent to the total reactive power consumption at the converter bridges. Reactive power Q, can be defined by

$$Q = S_L = V_{L_{RMS}} I_{L_{RMS}} \tag{5}$$

For each mode, RMS values for the inductor voltage and current are calculated. Fig.3 illustrates typical waveforms for v_L and i_L for mode 6. Reactive power definitions are given in Table III for all modes.

IV. TPS ANALYSIS GENERALISATION

The analysis presented in this paper can be generalised for all known phase shift modulation techniques. To illustrate this, the following examples are considered by applying the mode operational constraints defined in Table I.

- ***Conventional phase shift (CPS)*** **[13]:** This is defined by D_1=1, D_2=1. Applying this definition to modes 6 and 6' yields $0 \le D_3 \le 1$. CPS is therefore fully achieved with these two modes.
- ***Dual phase shift (DPS)*** **[6, 19]:** This is characterized by D_1=D_2=D. Applying this definition to modes 6 and 6' yields $D \ge 0.5$ and $1-D \le D_3 \le D$. This does not represent the complete control range for D.
  Considering modes 3 and 3', if D_1=D_2=D, therefore $D \le 0.5$ and $D \le D_3 \le 1-D$. Consequently, modes 3, 3', 6 and 6' can cover the whole operating range for DPS.
- ***Extended phase shift (EPS)*** **[20]:** This is defined by either bridge voltages being a full square wave with the other bridge voltage controlled to be a quasi-square wave. Considering modes 6 and 6', if
  - D_1=1, therefore $D_2 \ge 0$ and $1-D_2 \le D_3 \le 1$.

Table II: Inductor currents (i_L) for positive half cycle switching intervals normalized to $1/4f_sL$.

Modes	$i_L(t_0)$	$i_L(t_1)$	$i_L(t_2)$	$i_L(t_3)$
1	$-[V_1D_1 - nV_2D_2]$	$[-V_1D_1 + 2V_1D_3 + nV_2D_2]$	$[-V_1D_1 + 2V_1D_2 + 2V_1D_3 - nV_2D_2]$	$[V_1D_1 - nV_2D_2]$
1'	$-[V_1D_1 + nV_2D_2]$	$[-V_1D_1 + 2V_1D_3 - nV_2D_2]$	$[-V_1D_1 + 2V_1D_2 + 2V_1D_3 + nV_2D_2]$	$[V_1D_1 + nV_2D_2]$
2	$-[V_1D_1 - 2nV_2 + nV_2D_2 + 2nV_2D_3]$	$[V_1D_1 + 2nV_2D_1 - nV_2D_2 + 2nV_2 - 2nV_2D_3]$	$[V_1D_1 + nV_2D_2]$	$[V_1D_1 + nV_2D_2]$
2'	$-[V_1D_1 + 2nV_2 - nV_2D_2 - 2nV_2D_3]$	$[V_1D_1 - 2nV_2 - 2nV_2D_1 + nV_2D_2 + 2nV_2D_3]$	$[V_1D_1 - nV_2D_2]$	$[V_1D_1 - nV_2D_2]$
3	$-[V_1D_1 - nV_2D_2]$	$[V_1D_1 + nV_2D_2]$	$[V_1D_1 + nV_2D_2]$	$[V_1D_1 - nV_2D_2]$
3'	$-[V_1D_1 + nV_2D_2]$	$[V_1D_1 - nV_2D_2]$	$[V_1D_1 - nV_2D_2]$	$[V_1D_1 + nV_2D_2]$
4	$-[V_1D_1 - 2nV_2 + nV_2D_2 + 2nV_2D_3]$	$[-V_1D_1 - 2V_1 + 2V_1D_2 + nV_2D_2 + 2V_1D_3]$	$[V_1D_1 + nV_2D_2]$	$[V_1D_1 + nV_2D_2]$
4'	$-[V_1D_1 + 2nV_2 - nV_2D_2 - 2nV_2D_3]$	$[-V_1D_1 - 2V_1 + 2V_1D_2 + 2V_1D_3 - nV_2D_2]$	$[V_1D_1 - nV_2D_2]$	$[V_1D_1 - nV_2D_2]$
5	$-[V_1D_1 - nV_2D_2]$	$[-V_1D_1 + 2V_1D_3 + nV_2D_2]$	$[V_1D_1 - 2nV_2D_1 + nV_2D_2 + 2nV_2D_3]$	$[V_1D_1 - nV_2D_2]$
5'	$-[V_1D_1 + nV_2D_2]$	$[-V_1D_1 + 2V_1D_3 - nV_2D_2]$	$[V_1D_1 + 2nV_2D_1 - nV_2D_2 - 2nV_2D_3]$	$[V_1D_1 + nV_2D_2]$
6	$-[V_1D_1 + nV_2D_2 + 2nV_2D_3 - 2nV_2]$	$[-V_1D_1 + 2V_1D_2 + 2V_1D_3 + nV_2D_2 - 2V_1]$	$[-V_1D_1 + 2V_1D_3 + nV_2D_2]$	$[V_1D_1 - 2nV_2D_1 + nV_2D_2 + 2nV_2D_3]$
6'	$-[V_1D_1 - nV_2D_2 - 2nV_2D_3 + 2nV_2]$	$[-V_1D_1 + 2V_1D_2 + 2V_1D_3 - nV_2D_2 - 2V_1]$	$[-V_1D_1 + 2V_1D_3 - nV_2D_2]$	$[V_1D_1 + 2nV_2D_1 - nV_2D_2 - 2nV_2D_3]$

Table III: Constraints for operation of all switches under ZVS in the whole operating range & reactive power expressions.

	Mode 1	*Mode 1'*	*Mode 2*	*Mode 2'*
ZVS possible for all switches? Constraints	*NO* -	*YES* $i_L(t_0)<0, i_L(t_1)<0 \,\&\, i_L(t_2)>0$	*YES* $i_L(t_0)<0, i_L(t_1)>0 \,\&\, i_L(t_2)>0$	*YES* $i_L(t_0)<0, i_L(t_1)>0 \,\&\, i_L(t_2)<0$
Reactive power (Q)	$v_{rms} = \sqrt{V_1^2D_1 + n^2V_2^2D_2 - 2nV_1V_2D_2}$ $i_{rms} = \sqrt{\left\{\left[i_L^2(t_2)(1-D_1)\right] + \left[\frac{2f_sL}{3}\left\{\left[\frac{i_L^3(t_1)-i_L^3(t_0)}{V_1}\right] + \left[\frac{i_L^3(t_2)-i_L^3(t_1)}{V_1-nV_2}\right] + \left[\frac{i_L^3(t_3)-i_L^3(t_2)}{V_1}\right]\right\}\right]\right\}}$ $Q_1 = v_{rms1} \times i_{rms}$	$v_{rms1'} = \sqrt{V_1^2D_1 + n^2V_2^2D_2 + 2nV_1V_2D_2}$ $i_{rms1'} = \sqrt{\left\{\left[i_L^2(t_2)(1-D_1)\right] + \left[\frac{2f_sL}{3}\left\{\left[\frac{i_L^3(t_1)-i_L^3(t_0)}{V_1}\right] + \left[\frac{i_L^3(t_2)-i_L^3(t_1)}{V_1+nV_2}\right] + \left[\frac{i_L^3(t_3)-i_L^3(t_2)}{V_1}\right]\right\}\right]\right\}}$ $Q_{1'} = v_{rms1'} \times i_{rms1'}$	$v_{rms2} = \sqrt{V_1^2D_1 + n^2V_2^2D_2 + 2nV_1V_2D_1}$ $i_{rms2} = \sqrt{\left\{\left[i_L^2(t_2)(1-D_2)\right] + \left[\frac{2f_sL}{3}\left\{\left[\frac{i_L^3(t_1)-i_L^3(t_0)}{V_1+nV_2}\right] + \left[\frac{i_L^3(t_2)-i_L^3(t_1)}{nV_2}\right] + \left[\frac{i_L^3(t_0)+i_L^3(t_3)}{nV_2}\right]\right\}\right]\right\}}$ $Q_2 = v_{rms2} \times i_{rms2}$	$v_{rms2'} = \sqrt{V_1^2D_1 + n^2V_2^2D_2 - 2nV_1V_2D_1}$ $i_{rms2'} = \sqrt{\left\{\left[i_L^2(t_2)(1-D_2)\right] + \left[\frac{2f_sL}{3}\left\{\left[\frac{i_L^3(t_1)-i_L^3(t_0)}{V_1-nV_2}\right] - \left[\frac{i_L^3(t_2)-i_L^3(t_1)}{nV_2}\right] - \left[\frac{i_L^3(t_0)+i_L^3(t_3)}{nV_2}\right]\right\}\right]\right\}}$ $Q_{2'} = v_{rms2'} \times i_{rms2'}$
	Mode 3	***Mode 3'***	***Mode 4***	***Mode 4'***
ZVS possible for all switches? Constraints	*NO* -	*NO* -	*YES* $i_L(t_0)<0, i_L(t_1)>0 \,\&\, i_L(t_2)>0$	*NO* -
Reactive power (Q)	$v_{rms3} = \sqrt{V_1^2D_1 + n^2V_2^2D_2}$ $i_{rms3} = \sqrt{\left\{\left[\left[i_L^2(t_1)(D_3-D_1)\right] + \left[i_L^2(t_3)(1-D_2-D_3)\right]\right] + \left[\frac{2f_sL}{3}\left\{\left[\frac{i_L^3(t_1)-i_L^3(t_0)}{V_1}\right] - \left[\frac{i_L^3(t_2)-i_L^3(t_1)}{nV_2}\right]\right\}\right]\right\}}$ $Q_3 = v_{rms3} \times i_{rms3}$	$v_{rms3'} = \sqrt{V_1^2D_1 + n^2V_2^2D_2}$ $i_{rms3'} = \sqrt{\left\{\left[\left[i_L^2(t_1)(D_3-D_1)\right] + \left[i_L^2(t_3)(1-D_2-D_3)\right]\right] + \left[\frac{2f_sL}{3}\left\{\left[\frac{i_L^3(t_1)-i_L^3(t_0)}{V_1}\right] + \left[\frac{i_L^3(t_2)-i_L^3(t_1)}{nV_2}\right]\right\}\right]\right\}}$ $Q_{3'} = v_{rms3'} \times i_{rms3'}$	$v_{rms4} = \sqrt{V_1^2D_1 + n^2V_2^2D_2 + 2nV_1V_2(D_2+D_3-1)}$ $i_{rms4} = \sqrt{\left\{\left[i_L^2(t_2)(D_3-D_1)\right] + \left[\frac{2f_sL}{3}\left\{\left[\frac{i_L^3(t_1)-i_L^3(t_0)}{V_1+nV_2}\right] + \left[\frac{i_L^3(t_2)-i_L^3(t_1)}{V_1}\right] + \left[\frac{i_L^3(t_2)+i_L^3(t_0)}{nV_2}\right]\right\}\right]\right\}}$ $Q_4 = v_{rms4} \times i_{rms4}$	$v_{rms4'} = \sqrt{V_1^2D_1 + n^2V_2^2D_2 - 2nV_1V_2(D_2+D_3-1)}$ $i_{rms4'} = \sqrt{\left\{\left[\left[i_L^2(t_3)(D_3-D_1)\right] + \left[\frac{2f_sL}{3}\left\{\left[\frac{i_L^3(t_1)-i_L^3(t_0)}{V_1-nV_2}\right] + \left[\frac{i_L^3(t_2)-i_L^3(t_1)}{V_1}\right] - \left[\frac{i_L^3(t_3)+i_L^3(t_0)}{nV_2}\right]\right\}\right]\right\}}$ $Q_{4'} = v_{rms4'} \times i_{rms4'}$
	Mode 5	***Mode 5'***	***Mode 6***	***Mode 6'***
ZVS possible for all switches? Constraints	*NO* -	*YES* $i_L(t_0)<0, i_L(t_1)<0 \,\&\, i_L(t_2)>0$	*YES* $i_L(t_0)<0, i_L(t_1)>0, i_L(t_2)>0 \,\&\, i_L(t_3)>0$	*YES* $i_L(t_0)<0, i_L(t_1)<0, i_L(t_2)<0 \,\&\, i_L(t_3)>0$
Reactive power (Q)	$v_{rms5} = \sqrt{V_1^2D_1 + n^2V_2^2D_2 + 2nV_1V_2(D_3-D_1)}$ $i_{rms5} = \sqrt{\left\{\left[i_L^2(t_3)(1-D_2-D_3)\right] + \left[\frac{2f_sL}{3}\left\{\left[\frac{i_L^3(t_1)-i_L^3(t_0)}{V_1}\right] + \left[\frac{i_L^3(t_2)-i_L^3(t_1)}{V_1-nV_2}\right] - \left[\frac{i_L^3(t_3)-i_L^3(t_2)}{nV_2}\right]\right\}\right]\right\}}$ $Q_5 = v_{rms5} \times i_{rms5}$	$v_{rms5'} = \sqrt{V_1^2D_1 + n^2V_2^2D_2 + 2nV_1V_2(D_1-D_3)}$ $i_{rms5'} = \sqrt{\left\{\left[i_L^2(t_3)(1-D_2-D_3)\right] + \left[\frac{2f_sL}{3}\left\{\left[\frac{i_L^3(t_1)-i_L^3(t_0)}{V_1}\right] + \left[\frac{i_L^3(t_2)-i_L^3(t_1)}{V_1+nV_2}\right] + \left[\frac{i_L^3(t_3)-i_L^3(t_2)}{nV_2}\right]\right\}\right]\right\}}$ $Q_{5'} = v_{rms5'} \times i_{rms5'}$	$v_{rms6} = \sqrt{V_1^2D_1 + n^2V_2^2D_2 + 2nV_1V_2(D_2+2D_3-D_1-1)}$ $i_{rms6} = \sqrt{\left\{\left[\frac{2f_sL}{3}\left\{\left[\frac{i_L^3(t_1)-i_L^3(t_0)}{V_1+nV_2}\right] + \left[\frac{i_L^3(t_2)-i_L^3(t_1)}{V_1}\right] + \left[\frac{i_L^3(t_3)-i_L^3(t_2)}{V_1-nV_2}\right] + \left[\frac{i_L^3(t_0)+i_L^3(t_3)}{nV_2}\right]\right\}\right]\right\}}$ $Q_6 = v_{rms6} \times i_{rms6}$	$v_{rms6'} = \sqrt{V_1^2D_1 + n^2V_2^2D_2 + 2nV_1V_2(D_1-D_2-2D_3+1)}$ $i_{rms6'} = \sqrt{\left\{\left[\frac{2f_sL}{3}\left\{\left[\frac{i_L^3(t_1)-i_L^3(t_0)}{V_1-nV_2}\right] + \left[\frac{i_L^3(t_2)-i_L^3(t_1)}{V_1}\right] + \left[\frac{i_L^3(t_3)-i_L^3(t_2)}{V_1+nV_2}\right] - \left[\frac{i_L^3(t_0)+i_L^3(t_3)}{nV_2}\right]\right\}\right]\right\}}$ $Q_{6'} = v_{rms6'} \times i_{rms6'}$

- D_2=1, therefore $D_1 \geq 0$ and $0 \leq D_3 \leq D_1$.

EPS can therefore partially be achieved with modes 6 and 6'. Modes 1, 1', 2 and 2' cover the remaining EPS range of operation.

For Modes 1 and 1', if:

- D_1=1, therefore $D_2 \leq 1$ and $0 \leq D_3 \leq 1 - D_2$.

For Modes 2 and 2', if:

- D_2=1, therefore $D_1 \leq 1$ and $D_1 \leq D_3 \leq 1$.

V. SUMMARY AND CONCLUSIONS

Analysis of DAB converter using TPS was presented in this paper. Six switching modes and their complements have been identified using TPS control. Rather than using fundamental component approximation to determine average power transmitted, detailed analytical investigation was performed on all the switching modes. Moreover, based on the mode constraint, the power transfer range for each mode was derived. Inductor current which is crucial in the determination of DAB performances indices was computed for all the modes at each time intervals. ZVS constraints have been derived for all the modes in terms of possibility for all converter switches that can possibly operate under ZVS in different modes. A new accurate definition for DAB reactive power consumption is introduced based on the non-sinusoidal apparent power at the inductor. It is finally proven that the presented TPS analysis can be generalised to include all phase shift modulation techniques.

REFERENCES

[1] Jovcic, "Bidirectional high power DC transformer," IEEE Trans. Power Delivery, vol. 24, no. 4, pp. 2276-2283, Oct. 2009.

[2] R. W. De Doncker, D. M. Divan, and M. H. Kheraluwala, "A three phase soft-switched high power density dc/dc converter for high power applications," in Conf. Rec. IEEE IAS Annu. Meeting, Pittsburgh, PA,Oct. 2–7, 1988, pp. 796–805.

[3] G. Ortiz, J. Biela, D. Bortis, and J. Kolar, "1 Megawatt, 20 kHz, isolated, bidirectional 12kV to 1.2kV dc-dc converter for renewable energy applications," International Power Electronics Conference (IPEC), 2010, pp. 3212–3219,Jun. 2010.

[4] Krismer, F.; Kolar, J.W., "Accurate Power Loss Model Derivation of a High-Current Dual Active Bridge Converter for an Automotive Application," Industrial Electronics, IEEE Transactions on, vol.57, no.3, pp.881-891, March 2010.

[5] Y. Wang, S. W. H. de Haan, and J. A. Ferreira, "Optimal operating ranges of three modulation methods in dual active bridge converters," in IEEE 6th International Power Electronics and Motion Control Conference (IPEMC), 2009, pp. 1397–1401, 2009.

[6] H. Bai and C. Mi, "Eliminate reactive power and increase system efficiency of isolated bidirectional dual-active-bridge dc-dc converters using novel dual-phase-shift control," IEEE Transactions on Power Electronics, vol. 23, pp. 2905–2914, Nov. 2008.

[7] Jain, A.K.; Ayyanar, R "PWM Control of Dual Active Bridge: Comprehensive Analysis and Experimental Verification," IEEE transactions on power electronics, vol. 26, no. 4, April 2011.

[8] Garcia, G.O.,Ledhold, R.; Oliva, A.R. ; Balda, J.C. ; Barlow, F. , "Extending the ZVS Operating Range of Dual Active Bridge High-Power DC-DC Converters" IEEE Power Electronics Specialists Conference, 2006. PESC '06.

[9] Krismer, F.; Kolar, J.W.; "Closed Form Solution for Minimum Conduction Loss Modulation of DAB Converters," Power Electronics, IEEE Transactions on , vol.27, no.1, pp.174-188, Jan. 2012.

[10] G. Oggier, G. Garci, and A. Oliva, "Modulation strategy to operate the dual active bridge dc-dc converter under soft switching in the whole operating range," IEEE Transactions on Power Electronics, vol. 26, pp. 1228–1236, Apr. 2011.

[11] F. Krismer and J.W. Kolar, "Accurate small-signal model for the digital control of an automotive bidirectional dual active bridge,"IEEE Transactions on Power Electronics, vol. 24, pp. 2756–2768, Dec. 2009.

[12] B. Hua, C. C. Mi, and S. Gargies, "The short-time-scale transient processes in high-voltage and high-power isolated bidirectional dc-dc converters," IEEE Transactions on Power Electronics, vol. 23, pp. 2648–2656, Jun.2008.

[13] R. W. DeDoncker, D. M. Divan, and M. H. Kheraluwala, "A three phase soft-switched high power density dc-to-dc converter for high power applications," IEEE Trans. Industry Applications, vol. 27, no. 1, pp. 63-73, Jan./Feb. 1991

[14] W. Kuiyuan, C. W. de Silva, and W. G. Dunford, "Stability Analysis of Isolated Bidirectional Dual Active Full-Bridge DC-DC Converter With Triple Phase-Shift Control," Power Electronics, IEEE Transactions on, vol. 27, pp. 2007-2017, 2012.

[15] W. Huiqing, and X. Wei dong, "Bidirectional Dual-Active-Bridge DC-DC Converter with Triple-Phase-Shift Control," Applied Power Electronics Conference and Exposition (APEC) 2013, Twenty-Eighth Annual IEEE.

[16] J. Huang, Y.Wang, Y. Gao, W.Lei and Y. Li "Unified PWM Control to Minimize Conduction Losses Under ZVS in the Whole Operating Range of Dual Active Bridge Converters," Applied Power Electronics Conference and Exposition (APEC) 2013, Twenty-Eighth Annual IEEE.

[17] H. Wen, "Determination of the optimal sub-mode for bidirectional dual-active-bridge DC-DC converter with multi-phase-shift control," ECCE Asia Downunder (ECCE Asia), 2013 IEEE.

[18] Yongbin Chu and Shuo Wang, "Bi-directional isolated DC-DC converter with reactive power loss reduction for electric vehicle and grid support applications", in proc. Of IEEE Transportation Electrification conference, 18-20,Jun 2012.

[19] H. Bai and C. Mi, "Correction to "Eliminate Reactive Power and Increase System Efficiency of Isolated Bidirectional Dual-Active-Bridge DC–DC Converters Using Novel Dual-Phase-Shift Control", IEEE Transactions on Power Electronics, vol. 23, pp. 2905–2914, Sept. 2012.

[20] Biao Zhao, Qingguang Yu and Weixin Sun, "Extended-Phase-Shift Control of Isolated Bi-directional DC-DC Converter for Power Distribution in Microgrid", IEEE Transactions,on Power Electronics,2012.

[21] Rahman, M.I.; Jovcic, D.; Ahmed, K.H., "Reactive current optmisation for high power dual active bridge DC/DC converter," PowerTech (POWERTECH), 2013 IEEE Grenoble, vol., no., pp.1,6, 16-20 June 2013.